Dynamin:GTP Controls the Formation of Constricted Coated Pits, the Rate Limiting Step in Clathrin-mediated Endocytosis

Sanja Sever, Hanna Damke, and Sandra L. Schmid

Department of Cell Biology, The Scripps Research Institute, La Jolla, California 92037

Abstract. The GTPase dynamin is essential for receptor-mediated endocytosis, but its function remains controversial. A domain of dynamin, termed the GTPase effector domain (GED), controls dynamin's high stimulated rates of GTP hydrolysis by functioning as an assembly-dependent GAP. Dyn(K694A) and dyn(R725A) carry point mutations within GED resulting in reduced assembly stimulated GTPase activity. Biotinylated transferrin is more rapidly sequestered from avidin in cells transiently overexpressing either of these two activating mutants (Sever, S., A.B. Muhlberg, and S.L. Schmid. 1999. *Nature.* 398:481–486), suggesting that early events in receptor-mediated endocytosis are accelerated. Using stage-specific assays and morphological analyses of stably transformed cells, we have identified which events in clathrin-coated vesicle formation are accelerated by the overexpression of dyn(K694A) and dyn(R725A). Both mutants accelerate the formation of constricted coated pits, which we identify as the rate limiting step in endocytosis. Surprisingly, overexpression of dyn(R725A), whose primary defect is in stimulated GTP hydrolysis, but not dyn(K694A), whose primary defect is in self-assembly, inhibited membrane fission leading to coated vesicle release. Together, our data support a model in which dynamin functions like a classical GTPase as a key regulator of clathrin-mediated endocytosis.

Key words: dynamin • endocytosis • clathrin-coated vesicles • GTPase

Introduction

Clathrin-mediated endocytosis is one of the processes by which cells internalize macromolecules. Ultrastructural and biochemical analyses have established that the formation of clathrin-coated vesicles proceeds through several distinct steps (Schmid, 1997). Clathrin coat assembly is initiated by the binding of coat components to a docking site at the plasma membrane. Through the addition or rearrangement of coat constituents, the initially flat pit gains curvature, becoming progressively more invaginated, until the neck is constricted. Finally, membrane fission releases the coated vesicle, carrying its cargo into the cell interior (Gaidarov et al., 1999).

The large GTPase dynamin plays an essential role in clathrin-mediated endocytosis (for reviews see Warnock and Schmid, 1996; McNiven, 1998; Schmid et al., 1998), but its precise function in vesicle formation remains controversial (Kelly, 1999; Sever et al., 2000). Dynamin is a member of a growing subfamily of functionally diverse, high molecular mass GTPases that have atypically low affinities for GTP and high intrinsic rates of GTP hydrolysis. Dynamin will spontaneously self-assemble into supramolecular structures consisting of single rings and spirals upon dilution into low ionic strength buffers (Hinshaw and Schmid, 1995) or in the presence of artificial templates such as microtubules or acidic phospholipids (Shpetner and Vallee, 1989; Tuma and Collins, 1994). Self-assembly stimulates dynamin's basal GTPase activity 10–100-fold (Tuma and Collins, 1994; Warnock et al., 1996), and GTP hydrolysis drives dynamin disassembly (Maeda et al., 1992; Warnock et al., 1996).

In *Drosophila* bearing a temperature-sensitive allele of the dynamin homologue *shibire*, electron microscopy of the nerve terminals reveals the accumulation of endocytic pits, most of which are encircled at their necks by a single or double electron-dense band of similar dimensions to dynamin rings (Koenig and Ikeda, 1989). In mammalian cells, overexpression of dominant negative dynamin mutants inhibits endocytosis and leads to the accumulation of invaginated coated pits (Damke et al., 1994). Notably, dynamin collars have not been detected in nonneuronal cells, even in the *shibire* flies. In vitro studies have shown that when dynamin is assembled around lipid templates, GTP

Address correspondence to Sandra L. Schmid, Department of Cell Biology, The Scripps Research Institute, 10550 North Torrey Pines Road, La Jolla, CA 92037. Tel.: (858) 784-2311. Fax: (858) 784-9126. E-mail: slschmid@scripps.edu

The present address of S. Sever is Department of Biological Chemistry and Molecular Pharmacology, Harvard Medical School, Dana Farber Cancer Institute, Boston, MA 02115.

hydrolysis induces a conformational change which, depending on the composition of the lipid, causes either constriction of the dynamin spirals, resulting in vesiculation (Sweitzer and Hinshaw, 1998), or an increase in the spacing between the rungs of the assembled dynamin helix (Stowell et al., 1999). Together, these and other observations have led to various models (Hinshaw and Schmid, 1995; Warnock and Schmid, 1996; McNiven, 1998; Stowell et al., 1999) proposing that dynamin functions as a mechanochemical enzyme whose stimulated rate of GTP hydrolysis is required for pinching off vesicles from the plasma membrane (for review see Sever et al., 2000).

Dynamin mutants that are specifically defective in assembly stimulated GTPase activity (Sever et al., 1999) were designed to test its function in endocytosis. Dynamin's stimulated GTPase activity is controlled by an intramolecular GAP, encoded within dynamin's GTPase effector domain (GED,[1] amino acids 658–750) that becomes activated upon self-assembly (Muhlberg et al., 1997; Sever et al., 1999). A lysine residue, K694, is involved in intermolecular GED–GED interactions that occur upon self-assembly and are required for GAP activation; whereas an arginine residue, R725, participates more directly in catalysis (Sever et al., 1999). Substitution of either one of these residues with alanine specifically impairs the GAP-dependent, assembly stimulated rate of GTP hydrolysis, without affecting dynamin's basal GTPase rate. In the case of the dyn(R725A) mutant, the GAP defect is due to impaired catalytic activity, whereas in the case of the dyn(K694A) mutant, the defect is due to impaired self-assembly.

Unexpectedly, transient overexpression of either of these dynamin mutants accelerated the rate of receptor-mediated endocytosis as measured by the sequestration of biotinylated transferrin (B-Tfn) from avidin (Sever et al., 1999). These results challenged the view that dynamin acts as a mechanochemical enzyme because neither the maximal stimulated rate of GTP hydrolysis nor self-assembly appeared to be prerequisites for efficient endocytosis. Instead, because both of these activating mutants of dynamin are predicted to prolong dynamin in its GTP-bound form, these results suggested that, like other members of the GTPase superfamily, dynamin:GTP controls a rate-limiting step in endocytosis by recruiting a downstream partner.

Here, we report a detailed biochemical and morphological analysis of the functional consequences of overexpression of dyn(K694A) and dyn(R725A) in stably transformed cells aimed at addressing two unresolved questions. First, which event(s) in the formation of clathrin-coated vesicles are regulated by the GTP-bound form of dynamin? Second, given that dynamin:GTP is the active form, what is the role of rapid, assembly stimulated GTP hydrolysis? By using assays that distinguish between different steps in the formation of clathrin-coated vesicles, we show that both of the activating mutants accelerate the formation of constricted coated pits and more rapid sequestration of B-Tfn. However, overexpression of dyn (R725A), which is predicted to be defective in disassembly, decreased the rate of vesicle release. Together, our results suggest that dynamin:GTP controls the formation of constricted coated pits, and that the role of the stimulated rate of GTP-hydrolysis may be to switch dynamin off and release it from the membrane so that it does not impede membrane fission.

[1]*Abbreviations used in this paper:* BSS-Tfn, biotinylated transferrin; dyn, dynamin; GED, GTPase effector domain; MesNa, 2-mercaptoethanesulfonic acid; Tfn, transferrin; tet, tetracycline.

Materials and Methods

Reagents

The mouse monoclonal antitransferrin receptor antibody HTR.D65 was a gift from I. Trowbridge (Salk Institute, La Jolla, CA). Rhodamine-conjugated transferrin was purchased from Molecular Probes. Human differic transferrin (Tfn) was purchased from Boehringer. Tfn was biotinylated as previously described (Smythe et al., 1992). Colloidal gold (6 nm) and all other reagents used for EM were purchased from Electron Microscopy Sciences. D65 was conjugated to gold following standard protocols (Leunissen and DeMey, 1987). All other chemicals were reagent grade, unless otherwise specified.

Preparation of cDNA Constructs

The cDNAs for dyn(K694A) and dyn(R725A) were subcloned from the pcDNA vectors described previously (Sever et al., 1999) into the tetracycline (tet)-inducible expression plasmid pUHD10-3 containing HA-tagged (MQYDVPDYAH) wild-type dynamin (Damke et al., 1994). This construct was previously digested with NdeI and HindIII enzymes that removed the wild-type dynamin coding sequence, but preserved the HA tag within the vector. cDNA encoding the human TfnR was provided by Dr. Caroline Enns (Oregon University Health Sciences Center, Portland, OR), as previously described (Sever et al., 1999).

Generation of Stably Transformed Cells

The stable HeLa cell line, tTA-HeLa, expressing the chimeric tet-regulatable transcription activator was provided by H. Bujard (ZMBH, Heidelberg, Germany). Cells were maintained in DME supplemented with 10% (vol/vol) FBS, 100 U/ml each of penicillin and streptomycin and 400 μg/ml of active G418 (Geneticin; GIBCO BRL). The constructs pUHD10-3 encoding HA-tagged dyn(K694A) and dyn(R725A) were used to generate stably transformed tTA-HeLa cells with tightly regulated expression of dynamin as described previously (Damke et al., 1995). Puromycin was used as selectable marker.

Western Blot Analysis

For quantification of dynamin expression, cell lysates of equivalent numbers of cells were prepared for wild-type and all dynamin mutants, and were analyzed by Western blotting. For reliable quantification, different amounts of the cell lysates were loaded onto the SDS gel for all samples. The pan-dynamin antibody 748 (van der Bliek et al., 1993) was used to detect dynamin in comparison with endogenous dynamin in noninduced cells. Antigen–antibody complexes were visualized using HRP-conjugated goat anti–rabbit antibody and enhanced chemiluminescence (ECL; Amersham Pharmacia Biotech). The bands were quantified by densitometry.

Internalization Assays

Continuous Internalization Assay. Stably transformed tTA-HeLa cells were grown in the presence or absence of tetracycline for ~48 h to ~60% confluency. The cells were detached with PBS/5 mM EDTA at room temperature for 5 min, briefly rinsed, and resuspended in ice-cold PBS containing 1 mM $MgCl_2$, 1 mM $CaCl_2$, 0.2% BSA, and 5 mM glucose (PBS^{4+}) at 2×10^6 cells/ml. Biotinylated-transferrin (BSS-Tfn) was added to the suspension to a final concentration of 2 μg/ml BSS-Tfn and kept on ice. The cell suspension was split into 50-μl aliquots (corresponding to 2×10^5 cells) for continuous internalization of BSS-Tfn at 37°C for the indicated times. Returning the samples to ice stopped endocytosis. Internalization of the ligand was quantified after processing the samples for measuring

avidin inaccessibility or 2-mercaptoethanesulfonic acid (MesNa) resistance as described previously (Carter et al., 1993). Internalized BSS-Tfn was expressed as the percentage of total surface-bound BSS-Tfn at 4°C.

Single Round Internalization Assay. Cells were detached as described above, and, after the addition of BSS-Tfn, they were incubated on ice for 30 min. Cells were pelleted and the excess ligand was removed by aspiration. The cells were washed, and the pellets were resuspended at 2×10^6 cells/ml. The assay was performed as described above for the continuous internalization of BSS-Tfn.

Internalization of Rhodamine-Transferrin. Transformed tTA-HeLa cells were grown in the presence or absence of tet on glass coverslips for ~48 h to ~60% confluency. The cells were washed briefly in PBS and incubated with 20 μg/ml rhodamine-Tfn in PBS containing 1 mM $CaCl_2$, 1 mM $MgCl_2$, 5 mM glucose, and 0.2% BSA (PBS^{4+}) for 5 min. The cells were washed and fixed with 4% paraformaldehyde in PBS buffer for 30 min at room temperature, rinsed three times for 5 min with PBS, rinsed twice in dH_2O, and mounted with Fluoromount G (Electron Microscopy Sciences). The coverslips were viewed under an epifluorescence microscope (Axiophot; Carl Zeiss, Inc.), photographed using a digital camera, and prepared for publication using Adobe Photoshop 5.0.

Recycling of Tfn from Endosomal Compartments

Cells were incubated on 100-mm dishes for 60 min at 37°C with 8 μg/ml BSS-Tfn to reach equilibrium labeling. Plates were transferred to ice, washed several times with cold PBS, and surface-associated BSS-Tfn was masked with 50 μg/ml avidin for 15 min at 4°C. Avidin was quenched with biocytin (5 μg/ml). The cells were harvested from the plates by a 5-min incubation at 4°C with PBS/5 mM EDTA, and collected by centrifugation at 1,000 *g* for 5 min. Cells were resuspended at 4°C in PBS^{4+} containing 2 μg/ml unlabeled Tfn and incubated at 37°C for the indicated times. The BSS-Tfn that recycled to the cell surface during reincubation was again masked with avidin, and the cells were processed as described for the internalization assay. Results are expressed as the percentage of initial intracellular BSS-Tfn that remains inaccessible to avidin during reincubation.

Steady State Distribution

After binding of the ligand (4 μg/ml BSS-Tfn) to the cells at 0° or 37°C for 2 h, the cells were washed three times with cold PBS^{4+}. The amount of cell-associated ligand was determined by comparing the signal with the standard curve of known amounts of ligand using the ELISA assay. The proportion of the ligand on the cell surface was calculated as a ratio between the BSS-Tfn bound at 0° versus 37°C, as previously described (van der Sluijs et al., 1992).

Transmission Electron Microscopy

For conventional Epon sections, stably transformed cells were induced for 48 h in the absence of tet and grown to <75% confluency on 12-mm glass coverslips. After internalization of D65-gold (6 nm) in PBS^{4+} at 37°C for 30 min, the cells were washed and fixed in 2% glutaraldehyde in 100 mM sodium cacodylate buffer, pH 7.4 for 30 min at room temperature. Subsequently, the coverslips were washed for 1 h at room temperature in 100 mM sodium cacodylate buffer, pH 7.4 (four changes). The samples were postfixed with 1% OsO_4, 1% potassium ferrocyanide, 100 mM sodium cacodylate buffer, pH 7.4, for 1 h on ice, washed with four changes of dH_2O at room temperature, and stained with 2% uranyl acetate for 1 h at room temperature. After three washes in dH_2O at room temperature, the samples were dehydrated and embedded in Epon following standard protocols. Ultrathin sections were observed under an electron microscope (model CM10; Philips Sci.) at 80 kV. Quantitation of the coated pit accumulation was performed by photographing individual cell profiles at a low magnification (1,200×) to measure the surface length on negatives and then counting the number of coated pits and classifying their morphology at a high magnification (19,000×). At least 10 cell profiles were counted for each condition. Shallow pits were defined as having fully open mouths and U-shaped openings; deeply curved pits had narrow openings and were omega-shaped; and sealed pits were completely encircled by the coated membrane (see Fig. 5). In serial section analysis, sealed pits were invariably connected to the cell surface in neighboring sections, and were, therefore, grouped into the category of deep coated pits. Gold particles located on coated versus noncoated regions of the cell surface were also counted. The dimensions of randomly photographed deeply curved or sealed pits having clearly defined diameters were measured on EM negatives at 21,000× using a 15× magnifying glass and a ruler with 0.1-mm subdivisions.

Results

Conditional Expression of dyn(K694A) and dyn(R725A) in Stably Transformed Cells

Transient overexpression of the dynamin-1 mutants, dyn (K694A) and dyn(R725A), was shown to increase the rate of transferrin uptake into an avidin-inaccessible compartment in BHK cells (Sever et al., 1999). To characterize this novel phenotype in greater biochemical and morphological detail, we made stably transformed cell lines expressing each activating mutant. cDNAs encoding dyn(K694A) and dyn(R725A) with an NH_2-terminal HA epitope tag were inserted into a tet-regulatable expression vector (pUHD10-3), and were used to transform tTA-HeLa cells that express the tet-regulatable chimeric transcription activator (Gossen and Bujard, 1992; Damke et al., 1995). Clonal cell lines showing tight suppression of dynamin expression by tet and effective induction upon its removal, were selected and amplified, as previously described (Damke et al., 1994, 1995). As controls, we used stably transformed cells overexpressing wild-type dynamin-1 and a previously well characterized, dominant negative mutant dyn(K44A) (Damke et al., 1994). The level of overexpression was quantitated by Western blot analysis using the polyclonal antibody 748, which recognizes both neuronal and somatic isoforms of dynamin (Fig. 1 A, inset). Upon induction by removal of tet, dyn(wt) and dyn(K44A) were expressed at ~50- and >100-fold over endogenous dynamin-2, whereas dyn(K694A) and dyn(R725A) were expressed at ~10- and 6-fold over endogenous dynamin-2, respectively. Moreover, clonal cell lines expressing either

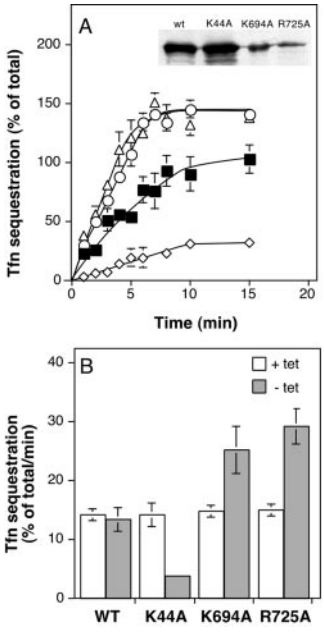

Figure 1. Transferrin internalization is increased in cells stably expressing the dyn (K694A) and dyn(R725A). (A) Cells expressing either wild-type dynamin (■), dyn (K44A) (◇), dyn(K694A) (○), or dyn(R725A) (△) were induced for 48 h by removal of tetracycline. The inset indicates the expression levels for exogenous dynamin from a single representative assay as analyzed by Western blotting. Internalization of transferrin (Tfn) was measured by incubating cells with 4 μg/ml B-Tfn for the indicated times at 37°C before measuring intracellular Tfn based on its inaccessibility to avidin (see Materials and Methods). (B) The initial rates of Tfn internalization, which were determined within the first 5 min of uptake for the induced cells, are shown (solid bars) relative to noninduced control cells (open bars). Results in both panels are the average ± SD of five independent experiments.

dyn(R725A) or dyn(K694A) were prone to lose dynamin expression over time in culture (data not shown; see Materials and Methods). The reasons for these different levels of expression and apparent instability are unknown. For all experiments shown here, cells were used within 3–4 wk of thawing, and dynamin expression levels were verified by Western blotting and immunofluorescence.

To follow receptor-mediated endocytosis in stably transformed cell lines, transferrin was biotinylated via a cleavable disulfide bond for use as a ligand (BSS-Tfn). Sequestration of BSS-Tfn into constricted coated pits or coated vesicles was measured by its acquired inaccessibility to exogenously added avidin. In agreement with our previous results in transiently transfected cells (Sever et al., 1999), overexpression of dyn(K694A) and dyn(R725A) increased the rate of BSS-Tfn sequestration when compared with cells overexpressing dyn(wt) (Fig. 1 A). Compared with noninduced cells or cells overexpressing dyn(wt), the rate of sequestration (i.e., percentage of surface-bound Tfn/min) increased approximately twofold in cells expressing either activating mutant and decreased by approximately fivefold in cells expressing the dominant negative mutant, dyn(K44A) (Fig. 1 B). The extent of increase in Tfn sequestration rates (twofold) is as great as would be expected given that other slow steps not directly controlled by dynamin, such as coated pit assembly, would become rate limiting. Together, these results support our original observation that impairment of the stimulated rate of GTP hydrolysis by dynamin increases the initial rate of Tfn sequestration.

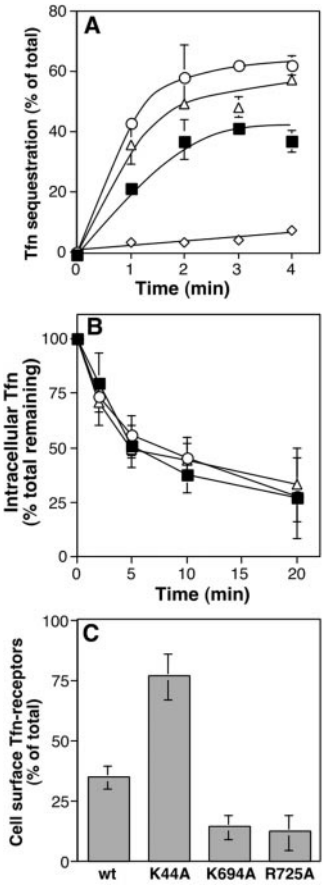

Figure 2. Effects of dynamin:GTP on the transferrin receptor cycle. Stably transformed tTA-HeLa cells expressing dyn(wt) (■), dyn(K44A) (◇), dyn(K694A) (○), or dyn(R725A) (△) were induced for ~48 h and analyzed in different assays. (A) Single-round kinetics of Tfn internalization were determined by first incubating cells with an excess of BSS-Tfn for 30 min on ice. After the unbound ligand was removed, internalization of prebound BSS-Tfn was determined at early time points by incubating cells at 37°C. (B) Recycling of Tfn receptors from endosomes was assessed by first loading cells with BSS-Tfn at 37°C to steady state. Surface-bound BSS-Tfn was masked by avidin at 4°C, and the recycling of intracellular BSS-Tfn was determined after incubation at 37°C for indicated times (see Materials and Methods). (C) Effects of dynamin mutants on the cellular distribution of the Tfn receptor was determined by allowing cells to bind BSS-Tfn on ice or at 37°C for 2 h. Unbound ligand was subsequently removed by extensive washing, and cell-associated BSS-Tfn was determined using the ELISA assay. The proportion of Tfn receptors on the surface (average ± SD, $n = 3$) was calculated as the ratio between the BSS-Tfn bound at 0 versus 37°C (van der Sluijs et al., 1992).

The Effects of Activating Mutants on the Transferrin Cycle

It remained possible that the observed increase in avidin-inaccessible BSS-Tfn was due to changes in the kinetics of the transferrin receptor recycling to the plasma membrane, rather than to the effects on the initial rate of endocytosis. To test this possibility, we examined the single-round kinetics of Tfn uptake. Cells were first incubated with an excess of BSS-Tfn for 30 min on ice to allow ligand binding, after which unbound BSS-Tfn was removed by extensive washing. Subsequently, cells were warmed to 37°C, and the sequestration of prebound ligand was measured at early time points. Both cell lines overexpressing the activating mutants exhibited an increase in the amount of sequestered Tfn (Fig. 2 A), in comparison with cells overexpressing dyn(wt). In contrast, Tfn uptake was severely inhibited by overexpression of the dominant negative mutant, dyn(K44A). Thus, the rate of a single round of Tfn uptake correlates well with the observed increase in the initial rate of endocytosis. This result also indirectly suggests that recycling of Tfn receptors from endosomes was not affected. To confirm this directly, the recycling endosomal compartments were loaded to steady state by incubating cells for 60 min at 37°C in the presence of saturating concentrations of BSS-Tfn. Surface-bound Tfn was masked by the addition of avidin at 4°C, and the cells were reincubated at 37°C to allow the exit of receptors with bound BSS-Tfn from the endosomal compartments to the cell surface. Newly exposed ligands were again masked with avidin. The results, shown in Fig. 2 B, establish that neither dyn(K694A) nor dyn(R725A) affected the kinetics of Tfn receptor recycling ($t_{1/2}$ ~8 min) from endosomes to the plasma membrane.

The ratio of intracellular to surface TfnR reflects their relative rates of internalization and recycling (Ciechanover et al., 1983); thus, selective increases in the rate of internalization should alter the steady state distribution of Tfn receptors. Therefore, we determined the fraction of TfnR at the cell surface (van der Sluijs et al., 1992) and found that cells overexpressing dyn(K694A) and dyn(R725A) displayed an approximately twofold decrease in the fraction of Tfn receptors distributed on the cell surface compared with dyn(wt) (Fig. 2 C). The altered steady state distribution of TfnR is also reflected in the increased plateau level of internalized Tfn seen in Fig. 1 A. In agreement with previous results using a different assay (Damke et al., 1994), overexpression of dyn(K44A) increased the number of receptors at the cell surface approximately twofold. Taken together, these results provide additional strong support that dynamin:GTP controls early events in receptor-mediated endocytosis.

Vesicle Formation Is Increased by dyn(K694A) but Not by dyn(R725A)

To determine which steps in coated vesicle formation are accelerated, we compared the effects of overexpression of dyn(K694A) and dyn(R725A) mutants using stage-specific assays based on the acquired inaccessibility of BSS-Tfn to probes of different sizes (Schmid and Carter, 1990; Schmid and Smythe, 1991; Carter et al., 1993). Ligands that are sequestered into constricted coated pits become inaccessible to bulky probes such as avidin, but remain accessible to the small, membrane impermeant–reducing agent, β-mercaptoethane sulfonic acid (MesNa). Only ligands that are internalized within a sealed clathrin-coated vesicle after release from the plasma membrane are inaccessible to MesNa. Under normal conditions, the rate and extent of endocytosis of the biotinylated ligand, as measured by using the two probes, is identical (Schmid and Carter, 1990; van der Bliek et al., 1993), suggesting that once a coated pit becomes constricted, membrane fission rapidly releases a coated vesicle. However, if membrane fission is selectively impaired and becomes rate-limiting, as was observed in cells depleted of ATP (Schmid and Carter, 1990), then the rate of sequestration of BSS-Tfn from the bulky probe will be faster than from the small probe.

To determine the effect of overexpression of dyn (K694A) and dyn(R725A) on membrane fission, we measured BSS-Tfn uptake into sealed coated vesicles using MesNa resistance. As previously reported (van der Bliek et al., 1993; Damke et al., 1994), overexpression of dyn(K44A) inhibited coated vesicle release (MesNa-resistance) as effectively as it inhibited the formation of constricted coated pits (avidin-inaccessibility; compare Fig. 1 A and 3, diamonds). Also, as expected, overexpression of dyn(K694A) increased the rate of accumulation of MesNa-resistant BSS-Tfn twofold compared with cells expressing dyn(wt) (Fig. 3 A, open circles), which is in close agreement to its effects on avidin inaccessibility (Fig. 1 A). In contrast, dyn(R725A) overexpression did not accelerate late events in endocytic-coated vesicle formation, and if anything was slightly inhibitory (Fig. 3 A, open triangles). Thus, for control cells (not shown, but see Schmid and Carter, 1990; Damke et al., 1994) or for cells overexpressing either dyn(wt) or dyn(K694A), the rate limiting step in coated vesicle formation is the formation of constricted coated pits. In contrast, for cells overexpressing dyn(R725A), membrane fission and coated vesicle release appear to be inhibited, so that these events become rate-limiting for endocytosis.

Dyn(R725A) and dyn(K694A) are expressed in stable cells at different levels (see above); therefore, it was theoretically possible that the observed difference in their phenotypes was due to differences in their expression levels. To test this possibility, we performed stage-specific assays under conditions in which both activating mutants were overexpressed at comparable levels using transient transfection assays (Sever et al., 1999). BHK cells were cotransfected with different dynamin constructs together with a construct encoding the human transferrin receptor to measure endocytosis of transferrin preferentially in the transfected population of cells. Western blot analysis showed that expression levels of dyn(wt), dyn(K44A), dyn(K694A), and dyn(R725A) were comparable (Fig. 3 B, inset) and >50-fold over the endogenous level (not shown). As was seen in the stably transformed cell lines (Fig. 1 A) and consistent with previous results (Sever et al., 1999), overexpression of either dyn(K694A) or dyn(R725A) significantly increased the rate of BSS-Tfn sequestration into avidin-inaccessible compartments (Fig. 3 B). However, only dyn(K694A) overexpression resulted in increased BSS-Tfn internalization into MesNa-resistant coated vesicles (Fig. 3 C). The rate of membrane fission and subsequent coated vesicle release was the same or lower in cells overexpressing dyn(R725A) compared with dyn(wt) (Fig. 3 C). Thus, the observed difference in phenotypes between the two activating dynamin mutants is due to differences in their enzymatic properties and not to expression levels.

The differential effects of overexpression of dyn (K694A) and dyn(R725A) on endocytosis were independently confirmed by immunofluorescence analysis following the internalization of rhodamine-conjugated Tfn. For

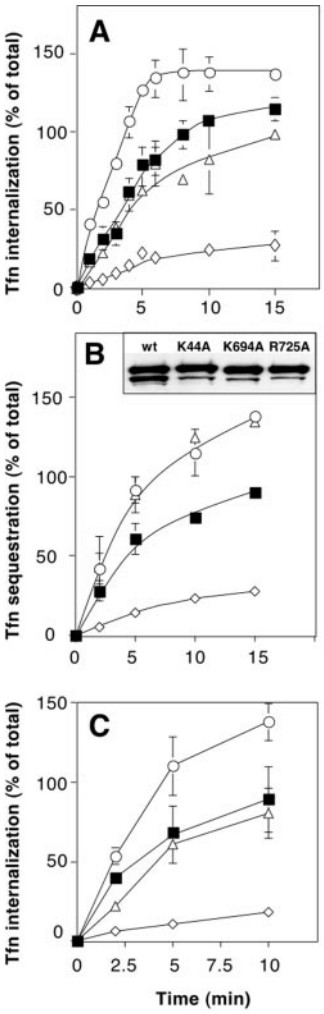

Figure 3. Membrane fission is inhibited in cells overexpressing dyn(R725A). (A) Stably transformed tTA-HeLa cells expressing dyn (wt) (■), dyn(K44A) (◇), dyn(K694A) (○), or dyn(R725A) (△) were induced for 48 h and internalization of Tfn into the sealed coated vesicles was assessed by MesNa resistance (see Materials and Methods). Results shown are the average ± SD of five independent experiments. (B and C) BHK cells were cotransfected with cDNAs encoding the human transferrin (Tfn) receptor and either wild-type dynamin (■), dyn(K44A) (◇), dyn(K694A) (○), or dyn(R725A) (△) and cultured for an additional 24 h before harvesting for endocytosis assays as described in Fig. 1. Inset in B shows Western blot analysis of the same number of BHK cells transiently transfected with cDNAs encoding different dynamin mutants. The lower band is a degradation product of dynamin seen at high levels of overexpression. The extent of BSS-Tfn internalization was assessed either by avidin accessibility (B) or MesNa resistance (C, see Materials and Methods). Shown are the average ± SD of three independent experiments with at least 60% transfection efficiency.

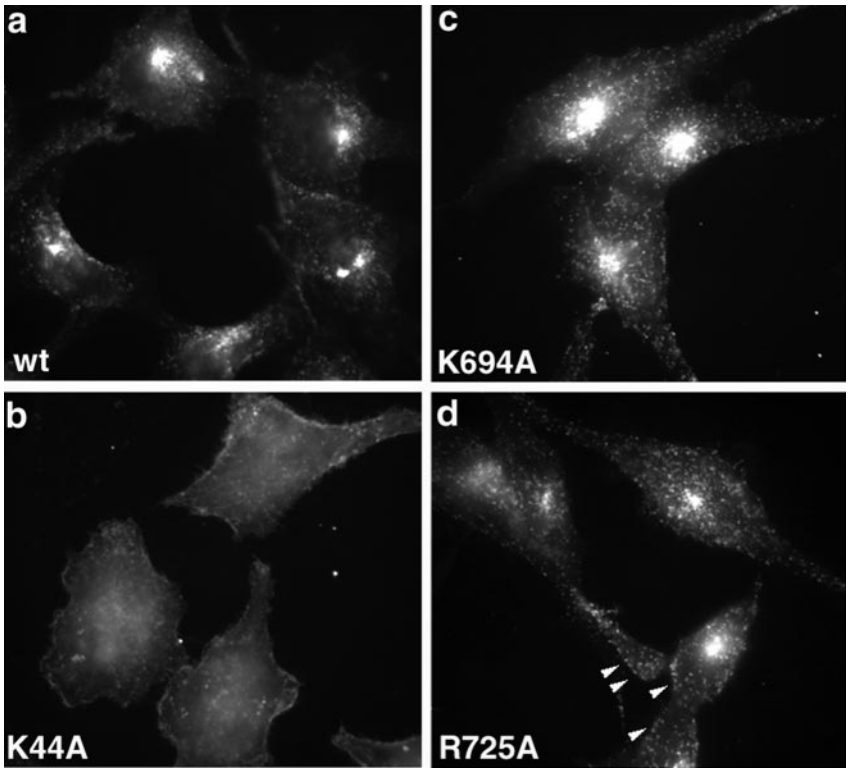

Figure 4. Effect of dynamin mutants on rhodamine-Tfn internalization. Stably transformed tTA-HeLa cells expressing dyn(wt) (a), dyn(K44A) (b), dyn(K694A) (c), or dyn(R725A) (d) were grown on coverslips for ~48 h, during which dynamin expression was induced by the removal of tet. Cells were incubated with rhodamine-Tfn for 5 min at 37°C before fixation and analysis by fluorescence microscopy.

these experiments, stably transformed cells overexpressing either wt or mutant dynamins were incubated with rhodamine-Tfn for 5 min at 37°C to assess early time points of internalization when effects were most striking (Figs. 1 A and 3 A). Rhodamine-Tfn was internalized more efficiently and accumulated to a greater extent in the perinuclear recycling endosomal compartment and in punctate early endosomal structures dispersed throughout the cytoplasm in cells expressing dyn(K694A) than in dyn(wt) cells (Fig. 4, compare C and A). In contrast, in cells overexpressing dyn(R725A), there was no detectable increase in Tfn accumulation in the perinuclear recycling endosomes as compared with dyn(wt) cells (Fig. 4, D versus A). However, rhodamine-Tfn appeared to accumulate in punctate structures at the cell periphery and at the level of the plasma membrane (Fig. 4 D, arrowheads). As expected, in cells overexpressing the dominant negative dyn(K44A), Tfn was not internalized and exhibited diffuse plasma membrane staining typical of surface-bound rhodamine-Tfn (Fig. 4, B). Thus, the immunofluorescence experiments correlate well with biochemical measurements, further establishing the difference between phenotypes induced by overexpression of dyn(K694A) and dyn (R725A).

Dynamin:GTP Controls the Rate of Coated Vesicle Formation

Both activating mutants of dynamin increased the rate of sequestration of ligand into avidin-inaccessible compartments. We can envisage several possibilities that could account for this effect. First, the individual coated pits and vesicles formed could be larger and, therefore, could accommodate more ligand per vesicle. Second, the total number of coated pits could increase, so that more vesicles are forming, albeit at the same rate per vesicle as in wt cells. Third, TfnR could be more effectively concentrated in coated pits, so that although individual coated vesicles form at the same rate, each carries a more concentrated load of cargo molecules. Finally, dynamin:GTP could increase the rate at which individual constricted coated pits are formed. To address these various possibilities, we undertook a detailed morphological analysis using thin section electron microscopy of the endocytic intermediates involved in the internalization of gold-conjugated anti–human Tfn-R mAb (D65-gold). Previous studies have established that this reagent is internalized identically to Tfn (Schmid and Smythe, 1991) and provides an excellent morphological tracer for EM analysis (Schmid and Smythe, 1991; Damke et al., 1994).

To uniformly label all endocytic intermediates, cells were incubated in the presence of D65-gold for 30 min at 37°C, fixed, embedded in Epon, and serial-sectioned for electron microscopy, as described in Materials and Methods. The representative micrographs in Fig. 5 and quantitation in Table I show that there was no significant change in the morphology or size of individual coated pits or coated vesicles in the cells overexpressing mutant dynamins as compared with wt dynamin. Similarly, the number of coat profiles in cells overexpressing dyn(K694A) or dyn(R725A) did not increase compared with dyn(wt) cells. Unexpectedly, there was an apparent decrease in the number of coated pits in dyn(R725A) cells, which might reflect either an indirect effect on the recycling of some component needed to initiate the coat assembly or a direct inhibitory effect of mutant dynamin overexpression on the

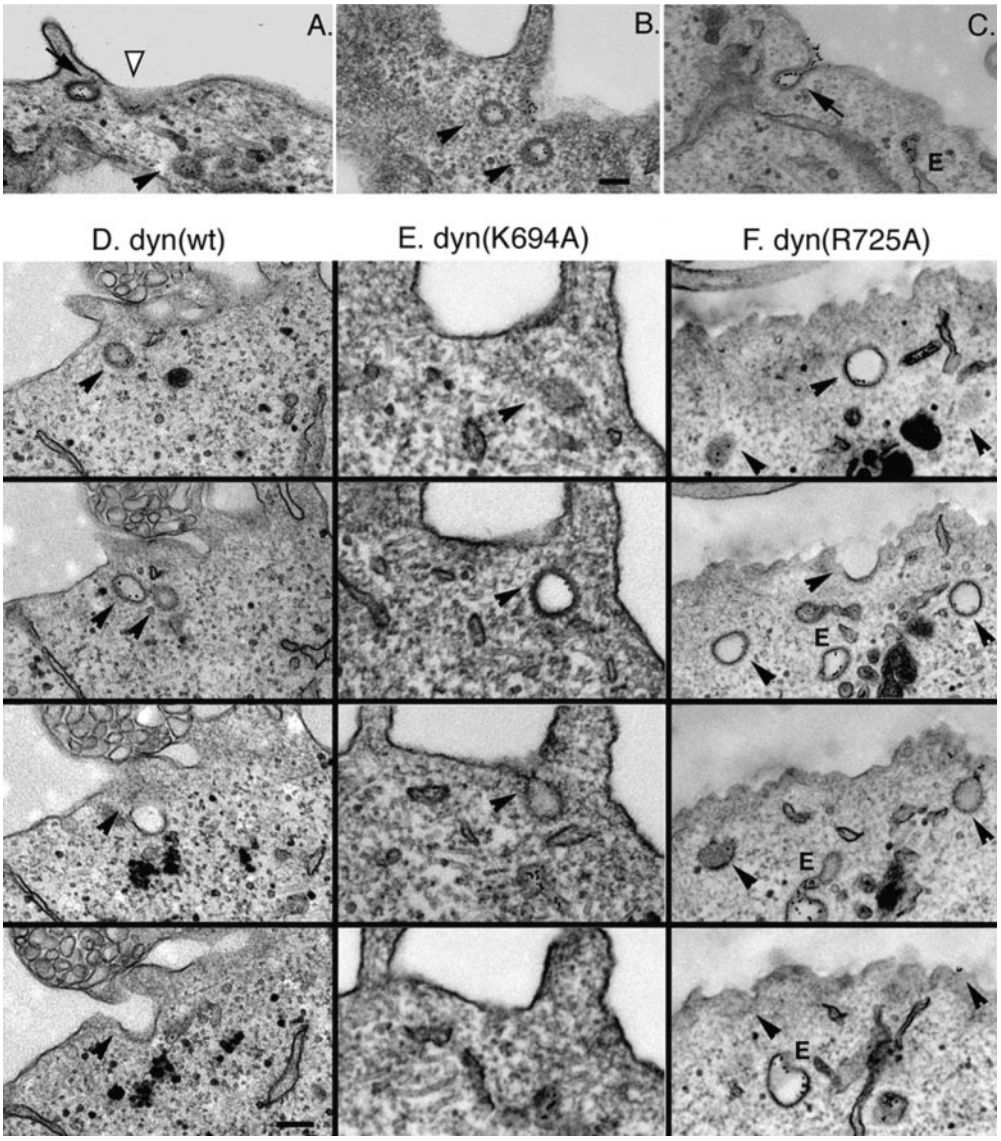

Figure 5. EM analysis of coated profiles in cells expressing wt and mutant dynamins. Transformed tTA-HeLa cells, which were induced to express either dyn(wt) (A and D), dyn (K694A) (B and E), or dyn(R725A) (C and F), were grown on coverslips. Cells were incubated with gold-conjugated monoclonal anti–human TfnR antibody (D65-gold) for 30 min at 37°C before fixation, staining, and embedding in Epon for thin section analysis. Open arrowhead (A) points to a shallow coated pit; closed arrowheads in (A–C) point to closed pits that are most likely open to the cell surface in subsequent sections (D–F); and arrows point to deep coated pits where openings are visible. E indicates endosomal structures containing D65-gold. Bar, 200 nm.

early stages of coated vesicle formation. Regardless, the increased rate of Tfn sequestration observed in dyn (K694A) and dyn(R725A) cells was not due to an increase in either the size or the number of coated pits formed.

We next examined the overall sorting efficiency of coated pits and coated vesicles by determining the percentage of surface-bound D65-gold associated with coated regions of the plasma membrane. Consistent with our biochemical measurements (Fig. 2 C), there was a decrease in the total amount of D65-gold bound to dynamin mutant compared to the dyn(wt) cells (Table I). However, for each cell type, 52% of surface-associated Tfn receptors were located in coated structures. Thus, the increased rate of Tfn sequestration was also not due to an increase in TfnR sorting efficiency. Interestingly, when the data were analyzed for individual coated pits and coated vesicles (Fig. 6, A–C), we found a statistically significant decrease in the number of gold particles/coated profile in cells expressing dyn (K694A) (mean = 2.3 gold particles/coated profile; n = 178; $P < 0.01$) relative to dyn(wt) cells (mean = 3.3 gold particles/coated profile; n = 176). These findings may reflect the faster rate of vesicle formation in dyn(K694A)

Table I. Quantitative Analysis of Coated Pits and TfnR Sorting Efficiencies

Cell type	Diameter of coated profiles	Coated profiles/ mm surface*	D65-gold/ mm surface*	Percent D65-gold in coated profiles
	nm			
Wild-type	160 ± 37 (n = 26)	116	588	52
Dyn(K694A)	161 ± 26 (n = 26)	97	407	52
Dyn(R725A)	151 ± 33 (n = 23)	68	460	52

*The membrane surface sampled was 966, 953, and 1,136 μm for wt, dyn(K694A), and dyn(R725A) cells, respectively.

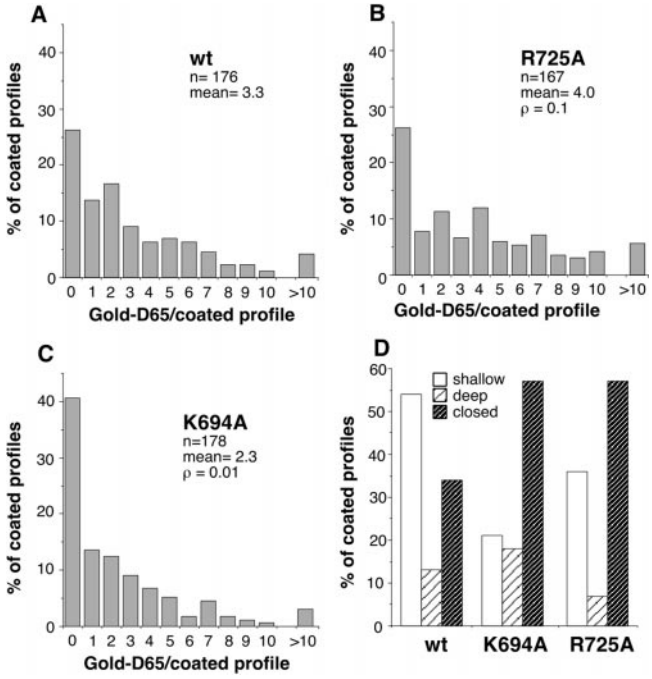

Figure 6. Quantitative analysis of TfnR sorting and endocytic intermediates in cells expressing wt and mutant dynamins. A–C show the distribution of coated profiles containing D65-gold for cells expressing dyn(wt) (A), dyn(K694A) (B), and dyn(R725A) (C). Cells overexpressing dyn(K694A) mutant show a statistically different distribution of gold particles relative to wt cells as assessed by the analysis of variance statistics (ANOVA). D shows the distribution of coated endocytic structures in wt and mutant cells. Quantitation was performed at the microscope as described in Materials and Methods. The total number of coated pits scored for this analysis was 68, 86, and 89 for wt, dyn(K694A) and dyn(R725A), respectively.

cells limiting the ability of individual pits to capture a full complement of cargo molecules. They also suggest that the actual rate of individual vesicle release in dyn(K694A) cells might be faster than the overall rates measured biochemically. The distribution of Tfn receptors in dyn (R725A) cells was not significantly different than in wild-type cells (mean = 4.0 gold particles/coated profile; n = 167; P = 0.1).

The strongest effect of overexpression of either dyn (K694A) or dyn(R725A) was a shift in the distribution of endocytic intermediates from early stages, seen as shallow, wide-mouthed pits (Fig. 5, A–C, open arrowheads) to later stages, seen as deeply invaginated pits still connected to the cell surface (Fig. 5, A–C, arrows) and closed vesicles with no detectable connection to the surface (Fig. 5, A–C, closed arrowheads). Limited serial section analysis (Fig. 5, D–F) revealed that all of the closed coated profiles examined had connections to the surface detected in subsequent sections. Our inability to detect free coated vesicles is consistent with their short lifetime (Gaidarov et al., 1999). Therefore, for the purposes of quantitation, we assumed that all of the closed profiles are actually coated pits, and scored them accordingly together with deeply invaginated coated pits (Fig. 6 D, striped bars). Quantitation of the data shows that deeply invaginated coated pits accumulate in dyn(K694A) and dyn(R725A) cells relative to wt cells at the expense of shallow coated pits (Fig. 6 D, open bars). Importantly, even though deeply invaginated coated pits accumulate in dyn(K694A) and dyn(R725A) cells, we were unable to distinguish by EM a particular structural intermediate as corresponding to the biochemically defined constricted coated pit. Whether the formation of a constricted coated pit corresponds to an acute narrowing of the opening or a more active process of priming, which is not distinguishable by EM, needs to be determined. Nonetheless, these morphological data establish that neither of the two activating mutants of dynamin induce the formation of novel endocytic structures, nor do they affect the dimensions or sorting efficiency of coated vesicles. Therefore, we conclude that dynamin:GTP increases the rate of formation of individual coated vesicles.

Discussion

Dynamin:GTP Regulates Coated Pit Invagination and Constriction

We have confirmed and extended previous observations (Sever et al., 1999) that early events in receptor-mediated endocytosis are accelerated in cells overexpressing novel activating mutants of dynamin selectively impaired in assembly stimulated GTP hydrolysis. Here, we show that overexpression of either dyn(K694A) or dyn(R725A) specifically increases the rate of formation of constricted coated pits. Our results identify this as being the rate limiting step in clathrin-mediated endocytosis. Biochemical analysis as well as morphological studies reported here and elsewhere (Pypaert et al., 1987; Schmid and Carter, 1990; Damke et al., 1994; Naim et al., 1995) are in agreement with this interpretation. The most prevalent intermediates in endocytic-coated vesicle formation in nonperturbed, wild-type cells are shallow and invaginated coated pits that remain fully open to the extracellular environment, indicating that an event subsequent to the formation of these intermediates is rate limiting. Overexpression of dynamin:GTP in cells shifts this steady state distribution from shallow to deeply invaginated pits, suggesting that dynamin may regulate membrane invagination and morphogenesis in vivo. This possibility is consistent with the phenotype of *shibire*^{ts} flies. When maintained at the nonpermissive temperature, endocytic pits that accumulate in *shibire*^{ts} flies remain accessible to the bulky probe, HRP-conjugated WGA (Kosaka and Ikeda, 1983). Importantly, turning on dynamin function upon return to the permissive temperature leads to rapid membrane invagination and not, as might be expected, to the formation of many small vesicles (Koenig and Ikeda, 1989, 1996). This observation prompted the suggestion (Roos and Kelly, 1997) that dynamin controls membrane morphogenesis, specifically membrane invagination, rather than membrane fission. Our results are in agreement with this hypothesis.

Dynamin is a member of a subfamily of large GTPases that are conserved between yeast, plants, and higher eukaryotes (van der Bliek, 1999). The family includes dynamin and the yeast vps1p, which play roles in vesicular transport, and dnm1p, which regulates mitochondrial fission (Bleazard et al., 1999; Labrousse et al., 1999). How-

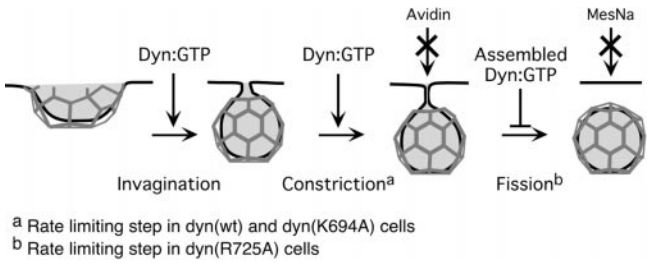

Figure 7. Kinetic model for the role of dynamin:GTP in endocytosis. Shown are the rate limiting steps in coated vesicle formation measured in cells overexpressing wt and mutant dynamins as detected biochemically. Our results suggest that the rate limiting step controlled by dynamin:GTP is the formation of the constricted pit needed to prime emerging vesicles for fission. Once the pit becomes constricted (or primed), it is rapidly consumed in the fission step to release a coated vesicle. Overexpression of dyn(K694A), which is impaired in self-assembly, increased the rate of formation of constricted coated pits and, correspondingly, the overall rate of endocytic-coated vesicle formation. In contrast, overexpression of the dyn(R725A), which is defective in GTP hydrolysis–triggered disassembly, increased the rate of formation of constricted coated pits without increasing the rate of coated vesicle release, so that membrane fission became rate-limiting. This suggests that assembled, GTPase–defective dynamin inhibits membrane fission.

ever, it also includes phragmoplastin, which is involved in membrane fusion during cell plate formation (Gu and Verma, 1997). Thus, while it appears that these enzymes perform opposite functions, this contradiction could be resolved if these dynamin families act as regulators of membrane morphogenesis, perhaps involved in priming membranes for either fission or fusion.

The Role of Stimulated GTP Hydrolysis in Membrane Fission

Both activating mutants accelerate the formation of constricted coated pits, which in wild-type cells is the rate limiting step in endocytosis (Fig. 7). As expected, by accelerating the rate limiting step, dyn(K694A) overexpression resulted in a corresponding increase in the overall rate of coated vesicle formation. Despite the twofold increase in the rate of formation of constricted coated pits in dyn (K694A) cells, this step remains rate limiting because it determines the rate of coated vesicle formation. Whether dyn(K694A) overexpression also positively regulates the rate of membrane fission remains to be determined. In contrast, the overall rate of coated vesicle formation was slightly slower in cells overexpressing dyn(R725A) compared with dyn(wt) cells. Thus, in dyn(R725A) cells, late events involving membrane fission and leading to vesicle release must have become rate limiting (Fig. 7). These results establish that rather than stimulating membrane fission, overexpression of dyn(R725A) inhibits membrane fission (Fig. 7). It should be noted that dyn(R725A) shows partial stimulated GTPase activity (approximately sixfold reduced relative to wt; Sever et al., 1999) and, although it cannot be assessed directly, it is likely that the extent of inhibition of the rate of membrane fission is in this range. However, even in the dyn(R725A) cells, we were unable to detect the accumulation of a structural intermediate corresponding to the biochemically defined constricted coated pit, suggesting that once such an intermediate forms, it is rapidly consumed, through membrane fission, leading to the release of coated vesicles.

The inhibitory effect of dyn(R725A) might suggest that dynamin's stimulated rate of GTP hydrolysis is important for efficient membrane fission, however, this interpretation is inconsistent with the stimulatory effect of the dyn(K694A) mutant, which is also defective in assembly stimulated GTPase activity. How can the differential effects of these two mutants be reconciled? Although both dyn(K694A) and dyn(R725) are defective in assembly stimulated GTPase activity, the primary biochemical defect of dyn(K694A) is its impaired ability to self-assemble (Sever et al., 1999). In contrast, dyn(R725A) assembles as effectively as wt and its primary defect is in the catalytic mechanism required for efficient GTP hydrolysis. GTP hydrolysis by dynamin triggers disassembly: it releases assembled dynamin from microtubules (Shpetner and Vallee, 1989; Maeda et al., 1992) and triggers disassembly of previously assembled dynamin in vitro (Warnock et al., 1997). Conversely, self-assembly of purified dynamin in vitro is promoted by GTPγS and GDP:AlF_4^- (Takei et al., 1995; Carr and Hinshaw, 1997). Based on these considerations, we suggest that the dyn(R725A) mutant may be defective in its rate of GTP-triggered disassembly. If so, one model to explain the differential phenotype induced by these two activating mutants is that the inhibitory effect of dyn(R725A) is due to its impaired disassembly such that membrane fission is inhibited in vivo when the lifetime of assembled dynamin is prolonged. In this case, the role of the stimulated rate of GTP hydrolysis could be to switch off dynamin and remove it from its site of action so that the subsequent fission step can occur.

Another possible consequence of the disassembly defect in dyn(R725A) cells would be that neither dynamin nor other components of the endocytic machinery that might interact with assembled dynamin are effectively recycled. The reduced availability of proteins required for earlier stages of endocytic vesicle formation might account for the reduced numbers or coat pits detected in dyn(R725A) cells and the slightly reduced accumulation of deeply invaginated coated pits compared with cells overexpressing dyn(K694A). Further studies are needed to determine whether these more subtle effects of overexpression of dyn(R725A) are direct or indirect.

This model for the dyn(R725A) phenotype suggests that the stimulated rate of GTP hydrolysis, dynamin disassembly, and the fission reaction are temporally very tightly coupled. While our understanding of these processes will require the elucidation of the fission reaction on the molecular level, our model for the specific phenotype of dyn(R725A) reconciles the apparently contradictory results that prolonging the lifetime of dynamin:GTP can increase the rate of endocytosis in vivo, but GTPγS inhibits endocytosis in vitro (Carter et al., 1993, Takei et al., 1995). Our data suggest that the late inhibitory effects of GTPγS on vesicle release might be partially due to the stabilization of assembled dynamin. Moreover, GTPγS will inhibit both dynamin's stimulated and basal rates of GTP hydrolysis. It is possible that the two different rates of GTP hydrolysis play very different roles in vivo. Indeed, it is well

established that GTPase domain mutants of dynamin that are defective in GTP binding and/or hydrolysis are potent inhibitors of receptor-mediated endocytosis (Herskovitz et al., 1993; van der Bliek et al., 1993).

Dynamin Collars and Endocytosis

The stimulatory effect of dyn(K694A) argues that dynamin self-assembly is not rate limiting for the formation of constricted coated pits. This conclusion is inconsistent with the original proposal that dynamin self-assembly into a helical collar plays a direct role in the formation of a constricted pit (Hinshaw and Schmid, 1995; Warnock and Schmid, 1996). The most straight-forward interpretation of the in vivo phenotype of dyn(K694A) cells would suggest that self-assembly is also not a prerequisite for dynamin function in coated vesicle formation. One caveat to this conclusion is that we are unable to demonstrate whether dyn(K694A) is able to self-assemble at all in vivo, and, if so, to what extent. It is conceivable that upstream events (e.g., the formation of a thin membrane neck) might provide a template for dyn(K694A) assembly in vivo, just as microtubules can in vitro. If dyn(K694A) self-assembly is allowed to occur in vitro around an artificial template such as a microtubule, then the stimulated GTPase activity of this mutant approaches wild-type levels (Sever et al., 1999). The fact that overexpression of dyn(K694A) increases the rate of coated vesicle formation suggests that its primary defect in self-assembly is indeed manifested in vivo. Thus, a more complex scenario to explain our observations would be that the defect in dyn(K694A) assembly is manifested at earlier stages in coated vesicle formation, thus, resulting in a prolonged lifetime of dynamin:GTP and increased rates of coated pit constriction. When the narrowing membranous neck reaches the appropriate dimensions dyn(K694A) self-assembly is initiated, and rapid GTP hydrolysis promotes efficient completion of the fission reaction. Further work is needed to resolve these two possibilities. Regardless, the phenotype induced by dyn(K694A) overexpression strongly suggests that dynamin self-assembly is not rate-limiting for endocytosis.

Our model, that overexpression of dyn(R725A) inhibits membrane fission because of impaired disassembly, would predict that collared pits might accumulate in these cells. In contrast to this prediction, in observing >160 coated pits in dyn(R725A) cells and >800 coated pits in total, we were unable to detect a collared pit, even with serial section analysis. These results are in agreement with the fact that observations of dynamin collars have not been reported in nonneuronal cells, even those expressing the same dynamin mutant that forms collars in neurons (Koenig and Ikeda, 1990; Tsuruhara et al., 1990; Damke et al., 1995; Baba et al., 1999). A recent structural study showed that when purified dynamin assembles onto liposomes in the presence of GTPγS, the dynamin spirals detectable by negative staining are not detectable by thin section EM (Takei et al., 1999). However, electron-dense spirals become detectable when dynamin coassembles with amphiphysin. Based on these results, it is possible that the assembly of other, perhaps neuron-specific, proteins accounts for the electron-dense bands specifically detected at synapses in *shibire*^{ts} flies. Importantly, dyn (R725A) is a kinetic mutant that slows but does not block membrane fission. In fact, the overall rate of Tfn endocytosis observed in dyn(R725A) cells is comparable to that observed in wt cells. Thus, it remains possible that the dynamin collars assembled by this mutant are still too short-lived to be readily detected.

Downstream Partners of Dynamin:GTP Mediate Coated Pit Invagination Leading to Constriction

Our analysis of dynamin function in vivo strongly argues that downstream partners of dynamin:GTP play direct roles in forming constricted coated pits. Several Src homology-3 domain–containing proteins also have been identified to interact with dynamin (Schmid et al., 1998) and to function in coated vesicle formation (Wigge et al., 1997; Simpson et al., 1999). One of these proteins, endophilin, appears to play a direct role in generating membrane curvature at both early and late stages in coated vesicle formation (Ringstad et al., 1999; Schmidt et al., 1999). Its recently identified lysophosphatidic acid acyl transferase activity (Schmidt et al., 1999) can alter the lipid composition of the membrane and provides a mechanism for inducing negative membrane curvature in the cytoplasmic leaflet of the bilayer needed to form a narrow neck. Endophilin's lipid modifying activity may also play a direct role in priming emerging coated vesicles for fission. Whether endophilin is a downstream effector of dynamin remains to be determined. Nevertheless, our work strongly suggests that dynamin acts as a regulatory GTPase to control downstream partners that mediate the rate limiting event in endocytosis.

We thank Laura Terlecky for help in generating the stable cell lines used in these studies and Richard Jacobs (Salk Institute) for skilled preparation of serial sections and electron microscopy. We thank members of the Schmid lab for many helpful discussions and for careful reading of the manuscript.

With the assistance of Chris Hofeditz and Tammie McQuistan, extensive use was made of the EM Core Facility led by Dr. M. Farquhar under the auspices of National Cancer Institute grant CA58689. S.L. Schmid was supported by the National Institutes of Health grant GM42455 and S. Sever by a Postdoctoral Fellowship from the American Cancer Society (California Division). This is The Scripps Research Institute manuscript No. 13135-CB.

Submitted: 1 May 2000
Revised: 14 July 2000
Accepted: 14 July 2000

References

Baba, T., H. Ueda, N. Terada, Y. Fujii, and S. Ohno. 1999. Immunocytochemical study of endocytotic structures accumulated in HeLa cells transformed with a temperature-sensitive mutant of dynamin. *J. Histochem. Cytochem.* 47:637–648.

Bleazard, W., J.M. McCaffery, E.J. King, S. Bale, A. Mozdy, Q. Tieu, J. Nunnari, and J.M. Shaw. 1999. The dynamin-related GTPase Dnm1 regulates mitochondrial fission in yeast. *Nat. Cell Biol.* 1:298–304.

Carr, J.F., and J.E. Hinshaw. 1997. Dynamin assembles into spirals under physiological salt conditions upon the addition of GDP and gamma-phosphate analogues. *J. Biol. Chem.* 272:28030–28035.

Carter, L.L., T.E. Redelmeier, L.A. Woollenweber, and S.L. Schmid. 1993. Multiple GTP-binding proteins participate in clathrin-coated vesicle-mediated endocytosis. *J. Cell Biol.* 120:37–45.

Ciechanover, A., A.L. Schwartz, A. Dautry-Varsat, and H.F. Lodish. 1983. Kinetics of internalization and recycling of transferrin and the transferrin receptor in a human hepatoma cell line. Effect of lysosomotropic agents. *J. Biol. Chem.* 258:9681–9689.

Damke, H., T. Baba, D.E. Warnock, and S.L. Schmid. 1994. Induction of mutant dynamin specifically blocks endocytic coated vesicle formation. *J. Cell Biol.* 127:915–934.

Damke, H., S. Freundlieb, M. Gossen, H. Bujard, and S.L. Schmid. 1995. Tightly regulated and inducible expression of a dominant interfering dynamin mutant in stably transformed HeLa cells. *Methods Enzymol.* 257:209–221.

Gaidarov, I., F. Santini, R.A. Warren, and J.H. Keen. 1999. Spatial control of coated pit dynamics in living cells. *Nat. Cell Biol.* 1:1–7.

Gossen, M., and H. Bujard. 1992. Tight control of gene expression in mammalian cells by tetracycline-responsive promoters. *Proc. Natl. Acad. Sci. USA*. 89:5547–5551.

Gu, X., and D.P. Verma. 1997. Dynamics of phragmoplastin in living cells during cell plate formation and uncoupling of cell elongation from the plane of cell division. *Plant Cell*. 9:157–169.

Herskovits, J.S., C.C. Burgess, R.A. Obar, and R.B. Vallee. 1993. Effects of mutant rat dynamin on endocytosis. *J. Cell Biol.* 122:565–578.

Hinshaw, J.E., and S.L. Schmid. 1995. Dynamin self assembles into rings suggesting a mechanism for coated vesicle budding. *Nature*. 374:190–192.

Kelly, R. 1999. New twists for dynamin. *Nat. Cell Biol.* 1:E8–E9.

Koenig, J.H., and K. Ikeda. 1989. Disappearance and reformation of synaptic vesicle membrane upon transmitter release observed under reversible blockage of membrane retrieval. *J. Neurosci.* 9:3844–3860.

Koenig, J.H., and K. Ikeda. 1990. Transformational process of the endosomal compartment in nephrocytes of *Drosophila melanogaster*. *Cell Tissue Res.* 262:233–244.

Koenig, J.H., and K. Ikeda. 1996. Synaptic vesicles have two distinct recycling pathways. *J. Cell Biol.* 135:797–808.

Kosaka, T., and K. Ikeda. 1983. Reversible blockage of membrane retrieval and endocytosis in the garland cell of the temperature-sensitive mutant of *Drosophila melanogaster*, *shibire*^{ts1}. *J. Cell Biol.* 97:499–507.

Labrousse, A.M., M.D. Zappaterra, D.A. Rube, and A.M. van der Bliek. 1999. *C. elegans* dynamin-related protein DRP-1 controls severing of the mitochondrial outer membrane. *Mol. Cell*. 4:815–826.

Leunissen, J.L.M., and J.R. DeMey. 1987. Preparation of gold probes. *In* Immuno-gold Labeling in Cell Biology. A.J. Verkleij and J.L.M. Leunissen, editors. CRC Press Inc., Baton Rouge, LA. 3–16.

Maeda, K., T. Nakata, Y. Noda, R. Sato-Yoshitake, and N. Hirokawa. 1992. Interaction of dynamin with microtubules: its structure and GTPase activity investigated by using highly purified dynamin. *Mol. Biol. Cell*. 3:1181–1194.

McNiven, M.A. 1998. Dynamin: a molecular motor with pinchase action. *Cell*. 94:151–154.

Muhlberg, A.B., D.E. Warnock, and S.L. Schmid. 1997. Domain structure and intramolecular regulation of dynamin GTPase. *EMBO (Eur. Mol. Biol. Organ.) J.* 16:6676–6683.

Naim, H.Y., D.T. Dodds, C.B. Brewer, and M.G. Roth. 1995. Apical and basolateral coated pits of MDCK cells differ in their rates of maturation into coated vesicles, but not in the ability to distinguish between mutant hemagglutinin proteins with different internalization signals. *J. Cell Biol.* 129:1241–1250.

Pypaert, M., J.M. Lucocq, and G. Warren. 1987. Coated pits in interphase and mitotic A431 cells. *Eur. J. Cell Biol.* 45:23–29.

Ringstad, N., H. Gad, R. Löw, G. Di Paolo, L. Brodin, O. Shupliakov, and R. De Camilli. 1999. Endophilin/SH3p4 is required for the transition from early to late stages in clathrin-mediated synaptic vesicle endocytosis. *Neuron*. 24: 143–154.

Roos, J., and R. Kelly. 1997. Is dynamin really a "pinchase." *Trends Cell Biol.* 7:257–259.

Schmid, S.L. 1997. Clathrin-coated vesicle formation and protein sorting: an integrated process. *Annu. Rev. Biochem*. 66:511–548.

Schmid, S.L., M.A. McNiven, and P. De Camilli. 1998. Dynamin and its partners: a progress report. *Curr. Opin. Cell Biol.* 10:504–512.

Schmid, S.L., and L.L. Carter. 1990. ATP is required for receptor-mediated endocytosis in intact cells. *J. Cell Biol.* 111:2307–2318.

Schmid, S.L., and E. Smythe. 1991. Stage-specific assays for coated pit formation and coated vesicle budding in vitro. *J. Cell Biol.* 114:869–880.

Schmidt, A., M. Wolde, C. Thiele, W. Fest, H. Kratzin, A.V. Podtelejnikov, W. Witke, W.B. Huttner, and H.D. Soling. 1999. Endophilin I mediates synaptic vesicle formation by transfer of arachidonate to lysophosphatidic acid. *Nature*. 401:133–141.

Sever, S., A.B. Muhlberg, and S.L. Schmid. 1999. Impairment of dynamin's GAP domain stimulates receptor-mediated endocytosis. *Nature*. 398:481–486.

Sever, S., H. Damke, and S.L. Schmid. 2000. Garrotes, springs, ratchets and whips: putting dynamin models to the test. *Traffic*. 1:385–392.

Shpetner, H.S., and R.B. Vallee. 1989. Identification of dynamin, a novel mechanochemical enzyme that mediates interactions between microtubules. *Cell*. 59:421–432.

Simpson, F., N.K. Hussain, B. Qualmann, R.B. Kelly, B.K. Kay, P.S. McPherson, and S.L. Schmid. 1999. SH3-domain-containing proteins function at distinct steps in clathrin-coated vesicle formation. *Nat. Cell Biol.* 1:119–124.

Smythe, E., L.L. Carter, and S.L. Schmid. 1992. Cytosol- and clathrin-dependent stimulation of endocytosis in vitro by purified adaptors. *J. Cell Biol.* 119:1163–1171.

Stowell, M.H.B., B. Marks, P. Wigge, and H.T. McMahon. 1999. Nucleotide-dependent conformational changes in dynamin: evidence for a mechanochemical molecular spring. *Nat. Cell Biol.* 1:27–32.

Sweitzer, S., and J. Hinshaw. 1998. Dynamin undergoes a GTP-dependent conformational change causing vesiculation. *Cell*. 93:1021–1029.

Takei, K., P.S. McPherson, S.L. Schmid, and P. De Camilli. 1995. Tubular membrane invaginations coated by dynamin rings are induced by GTPγS in nerve terminals. *Nature*. 374:186–190.

Takei, K., V.I. Slepnev, V. Haucke, and P. De Camilli. 1999. Functional partnership between amphiphysin and dynamin in clathrin-mediated endocytosis. *Nat. Cell Biol.* 1:33–39.

Tsuruhara, T., J.H. Koenig, and K. Ikeda. 1990. Synchronized endocytosis studied in the oocyte of a temperature-sensitive mutant of *Drosophila melanogaster*. *Cell Tissue Res.* 259:199–207.

Tuma, P.L., and C.A. Collins. 1994. Activation of dynamin GTPase is a result of positive cooperativity. *J. Biol. Chem*. 269:30842–30847.

van der Bliek, A.M. 1999. Functional diversity in the dynamin family. *Trends Cell Biol*. 9:96–102.

van der Bliek, A.M., T.E. Redelmeier, H. Damke, E.J. Tisdale, E.M. Meyerowitz, and S.L. Schmid. 1993. Mutations in human dynamin block an intermediate stage in coated vesicle formation. *J. Cell Biol.* 122:553–563.

van der Sluijs, P., M. Hull, P. Webster, P. Male, B. Goud, and I. Mellman. 1992. The small GTP-binding protein rab4 controls an early sorting event on the endocytic pathway. *Cell*. 70:729–740.

Warnock, D.E., and S.L. Schmid. 1996. Dynamin GTPase, a force generating molecular switch. *Bioessays*. 18:885–893.

Warnock, D.E., T. Baba, and S.L. Schmid. 1997. Ubiquitously expressed dynamin-II has a higher intrinsic GTPase activity and a greater propensity for self-assembly than neuronal dynamin-I. *Mol. Biol. Cell*. 8:2553–2562.

Warnock, D.E., J.E. Hinshaw, and S.L. Schmid. 1996. Dynamin self assembly stimulates its GTPase activity. *J. Biol. Chem*. 271:22310–22314.

Wigge, P., Y. Vallis, and H.T. McMahon. 1997. Inhibition of receptor-mediated endocytosis by the amphiphysin SH3 domain. *Curr. Biol*. 7:554–560.